

## Two Populations of Glucocorticoid Receptor-Binding Sites in the Male Rat Hippocampal Genome

J. Annelies E. Polman, E. Ronald de Kloet, and Nicole A. Datson

Division of Medical Pharmacology (J.A.E.P., E.R.d.K., N.A.D.), Leiden/Amsterdam Center for Drug Research, Leiden University Medical Center, 2300 RC Leiden, The Netherlands

In the present study, genomic binding sites of glucocorticoid receptors (GR) were identified *in vivo* in the rat hippocampus applying chromatin immunoprecipitation followed by next-generation sequencing. We identified 2470 significant GR-binding sites (GBS) and were able to confirm GR binding to a random selection of these GBS covering a wide range of *P* values. Analysis of the genomic distribution of the significant GBS revealed a high prevalence of intragenic GBS. Gene ontology clusters involved in neuronal plasticity and other essential neuronal processes were over-represented among the genes harboring a GBS or located in the vicinity of a GBS. Male adrenalectomized rats were challenged with increasing doses of the GR agonist corticosterone (CORT) ranging from 3 to 3000  $\mu\text{g/kg}$ , resulting in clear differences in the GR-binding profile to individual GBS. Two groups of GBS could be distinguished: a low-CORT group that displayed GR binding across the full range of CORT concentrations, and a second high-CORT group that displayed significant GR binding only after administering the highest concentration of CORT. All validated GBS, in both the low-CORT and high-CORT groups, displayed mineralocorticoid receptor binding, which remained relatively constant from 30  $\mu\text{g/kg}$  CORT upward. Motif analysis revealed that almost all GBS contained a glucocorticoid response element resembling the consensus motif in literature. In addition, motifs corresponding with new potential GR-interacting proteins were identified, such as zinc finger and BTB domain containing 3 (Zbtb3) and CUP (CG11181 gene product from transcript CG11181-RB), which may be involved in GR-dependent transactivation and transrepression, respectively. In conclusion, our results highlight the existence of 2 populations of GBS in the rat hippocampal genome. (*Endocrinology* 154: 1832–1844, 2013)

**S**tress, an actual or perceived threat to homeostasis, activates a neuroendocrine cascade leading to the release of glucocorticoid (GC) stress hormones (cortisol in humans and corticosterone in rodents (both abbreviated as CORT) by the adrenal. In the brain, GC bind to mineralocorticoid receptors (MR) and GC receptors (GR). GR are abundantly expressed throughout the brain (1, 2), whereas MR have a much more restricted expression in predominantly limbic brain structures. GR have a relatively low affinity for their ligand ( $K_d = 2.5\text{nM}–5\text{nM}$ ), and are therefore activated when circulating GC levels increase, eg, during stress or at the circadian peak, whereas

brain MR are already activated under basal nonstress conditions ( $K_d = 0.5\text{nM}$ ) (3). GR and MR mediate complementary and different, sometimes opposing, actions of CORT. Although MR are involved in maintenance of neuronal excitability and basal activity of the stress system and onset of the stress reaction, GR activation results in suppression of excitability transiently raised by excitatory stimuli, recovery from stress, and behavioral adaptation. Their balanced activation is an important determinant of neuronal excitability, neuronal health, and stress responsiveness (4, 5).

MR and GR belong to the superfamily of ligand-activated nuclear receptors and are involved in the regulation

ISSN Print 0013-7227 ISSN Online 1945-7170

Printed in U.S.A.

Copyright © 2013 by The Endocrine Society

Received December 5, 2012. Accepted February 20, 2013.

First Published Online March 22, 2013

Abbreviations: ADX, adrenalectomy; ChIP-Seq, high-throughput sequencing combined with chromatin immunoprecipitation; CORT, cortisol or corticosterone; CUP, CG11181 gene product from transcript CG11181-RB; FDR, false discovery rate; GBS, GR-binding site; GC, glucocorticoid; GR, GC receptor; GRE, glucocorticoid-responsive element; MACS, model-based analysis of ChIP-Seq; MR, mineralocorticoid receptor; MT2a, metallothionein 2A; mTOR, mammalian target of rapamycin; Sox12, SRY-box containing gene 12; UTR, untranslated region; Zbtb3, zinc finger and BTB domain containing 3.

of gene transcription. GR dimers interact directly with 15-nucleotide glucocorticoid-responsive elements (GRE) that are present in the DNA, to mostly stimulate transcription, a mechanism called transactivation (6). In addition, GR can bind other transcription factors such as activation protein-1, c-Jun N-terminal kinase, and nuclear factor- $\kappa$ B (7–9), thereby inhibiting their action, a mechanism known as transrepression.

The hippocampus, a brain structure important for learning, memory, mood, and regulation of the stress system, is a major target for GC and has high expression levels of both GR and MR (3, 4, 10). The balance of activated GR and MR influences not only cell birth and death but also other forms of neuroplasticity (5). Hippocampal neurons are particularly sensitive to GC and display a high degree of adaptive plasticity upon chronic GC exposure. Besides chronic exposure to GC, acute GC exposure can also affect structural plasticity in the brain. In the hippocampus, a few hours of intense stress reduced spine density on dendrites of CA3 neurons (11), whereas exposure to an acute restraint stress increased the density of spines on neurons in area CA1 of male rats (12). Besides structural changes, GC affect electrical properties of hippocampal neurons. Chronic stress or chronic CORT exposure suppresses hippocampal long-term potentiation (LTP), a lasting synaptic strengthening that likely underlies learning and memory formation (13–15). Consistent with these GR-mediated effects on structure and function, hippocampal GR regulate a wide variety of genes involved in diverse aspects of neuroplasticity (16).

Although studies into GC- and stress-responsive genes in the hippocampus have been insightful (16–19, 20), the identified genes are notoriously a mixture of primary and more downstream transcriptional responses, and it remains unclear whether GR actually bind to regulatory elements controlling expression of these genes. Technological advances in high-throughput sequencing combined with chromatin immunoprecipitation (ChIP-Seq) have made it possible to characterize genome-wide binding sites of GR in a variety of cell types (21–24), providing an unprecedented view on the motifs and genomic locations to which GR bind in different cellular contexts. However, so far today, the genome-wide binding sites of GR in vivo in the brain have not been characterized.

The aim of the current study was to identify genome-wide primary targets of GR in vivo in the hippocampus using ChIP-Seq and study whether activated GR bind to their primary targets in a dose-dependent way. In addition, we wanted to gain more knowledge on the genes that are located near genomic binding sites for GR and search for cross-talk partners of GR in the brain that might explain the cell type-specific targets of GR that are often

observed (21–24). Finally, we set out to investigate whether MR also bind to genomic binding sites of GR.

## Materials and Methods

### Experimental groups and tissue handling

For ChIP analysis, 8-week-old male Sprague Dawley rats (Harlan, Venray, The Netherlands) were housed in groups of 4 with food and water available ad libitum in a temperature (21°C) and humidity (55%) controlled room with a 12-hour light, 12-hour dark cycle (lights on at 7:30 AM). All experiments were conducted during the light phase. The rats were adrenalectomized as described before to completely deplete endogenous CORT levels and ensure there were no GR bound to the DNA (25). Three days after adrenalectomy (ADX), 4 groups of animals received an ip injection with 3, 30, 300, or 3000  $\mu$ g/kg CORT-hydroxypropyl-cyclodextrin complex while 1 group was left undisturbed ( $n = 6$  per group). All animals were decapitated after 1 hour for ChIP, and their hippocampi were isolated and processed for ChIP (see below). CORT levels in the blood 2 days after ADX and at the moment of decapitation were measured by RIA, showing that both the ADX operation was successful as well as a significant increase in CORT 1 or 3 hours after injection (Supplemental Figure 1, published on The Endocrine Society's Journals Online web site at <http://endo.endojournals.org>). Experiments were approved by the Local Committee for Animal Health, Ethics, and Research of the University of Leiden (DEC 06055 and 10044). Animal care was conducted in accordance with the European Commission Council Directive of November 1986 (86/609/EEC).

### Antibodies

Details on the antibodies used for ChIP are listed in Table 1. The antibodies used for GR and MR are commonly used in literature to study GR and MR in Western blot and immunohistochemical as well as immunoprecipitation studies in a wide variety of cells and tissues ([www.scbt.com](http://www.scbt.com)). We have successfully used the GR (H-300) antibody in the hippocampus for immunohistochemistry (26) and Western blot (27) and have obtained specific signals. Furthermore, we have used this antibody for ChIP and a ChIP-Seq study in undifferentiated and neuronally differentiated PC12 cells, respectively (24, 28). The MR H-300 antibody has been used for Western blot analysis in the guinea pig and rat hippocampus (29, 30).

### ChIP-Seq procedure

Because in vivo ChIP-Seq on brain tissue requires a minimum amount of chromatin as input, more than could be obtained from a single animal, 6 hippocampal hemispheres of 1 experimental group were pooled after shearing by sonication and divided in 2 equal portions, so that 2 ChIP procedures on identical samples (technical replicates) could be performed. This was done for both hemispheres, resulting in 4 ChIP samples that were stored at  $-80^{\circ}\text{C}$  until further processing.

The ChIP procedure was performed as described before (31). A detailed description of the ChIP procedure is available in Supplemental Document 1. Briefly, the samples were separately pre-cleared by incubating them with Sepharose A beads. After pre-

**Table 1.** Antibodies Used for the ChIP Study

Peptide/Protein Target	Antigen Sequence	Name of Antibody	Manufacturer, Catalog No., or Name of Source	Species Raised in Monoclonal or Polyclonal	Dilution Used
MR	Amino acids 1–300 at N terminus of human MR	MR antibody (H-300) X	Santa Cruz Biotechnology sc-11412X (ChIP application)	Rabbit polyclonal IgG	6 $\mu$ g/600 $\mu$ l
GR	Amino acids 121–420 within an internal region of human GR $\alpha$	GR antibody (H-300) X	Santa Cruz Biotechnology sc-8992X (ChIP application)	Rabbit polyclonal IgG	6 $\mu$ g/600 $\mu$ l

clearing, an input aliquot was taken of each sample to control for the amount of DNA used as input for the ChIP procedure. To reduce technical and biological variation, each sample was divided in 3 portions and incubated overnight at 4°C under continuous rotation with 6  $\mu$ g of either a GR, MR, or normal rabbit IgG antibody (Santa Cruz Biotechnology, Santa Cruz, California). Subsequently, the antibody-bound DNA fragments were isolated by incubating the samples with blocked protein A beads, after which the beads were washed and incubated with elution buffer to isolate the DNA-protein complexes. Finally, the DNA fragments were isolated by reverse cross-linking the samples, followed by ribonuclease treatment and purification on Nucleospin columns (Macherey-Nagel, Düren, Germany) (31). The immunoprecipitated samples were eluted in 50  $\mu$ l elution buffer.

For sequencing, IgG and GR ChIP samples of rats that received 3000  $\mu$ g/kg CORT were prepared according to the protocol supplied with the Illumina Genome Analyzer GA1 (Illumina, San Diego, California). In brief, the DNA fragments were blunted and ligated to sequencing adapters after which the DNA was amplified for 18 rounds of PCR. The DNA was electrophoresed on a 2% agarose gel, of which a region containing DNA fragments 100 to 500 base pairs (bp) in length was excised and the DNA extracted with the QIAGEN Gel Extraction Kit (QIAGEN, Hilden, Germany). DNA quality was checked on the Agilent Bioanalyzer (Waldbronn, Germany). Single end sequencing of the first 35 bp of the resulting DNA library was performed on the Illumina Genome Analyzer (Leiden Genome Technology Center, Leiden University Medical Center, Leiden University).

### Read alignment, peak calling, and mapping

We used the Burrows-Wheeler Aligner (32) to align 35-bp reads to the rat genome (rn4), controlling for unique tags, mismatch, and DNA gaps. Using BEDtools (33), we generated BED files that were used for model-based analysis of ChIP-Seq (MACS) (34) and wiggle files which could be used to visualize the reads on the UCSC genome browser (<http://genome.ucsc.edu>).

GR-binding sites (GBS) in the DNA relative to the nonspecific binding of the corresponding IgG ChIP-Seq sample were identified with the MACS peak caller (34). For peak calling, a  $P$  value cutoff of  $1.00 \times 10^{-5}$ , a model fold of 30 and a  $\lambda$  set of 1000/5000/10 000 were used to determine significant bound DNA regions. Per peak, a false discovery rate (FDR) was calculated by MACS.

Using Galaxy (<http://main.g2.bx.psu.edu/>) (35, 36), Refseq genes near the GBS were determined. As a reference genome, *Rattus norvegicus* 4 (rn4) was used. Data were visualized by

uploading wiggle files containing the raw ChIP-Seq data on the UCSC genome browser.

### Real-time quantitative PCR

For ChIP-Seq validation, a selection of GBS was validated by applying real-time quantitative PCR on immunoprecipitated chromatin. All cycle threshold values ranged from 25 to 32. The ChIP PCR signal was normalized by subtracting the amount of nonspecific binding of the IgG antibody in the same sample. Metallothionein 2A (MT2a), which has 2 well-documented GREs (37), served as a positive control for the ChIP. As a negative control, we analyzed GR binding to a nonbound GR region (exon 2 of the myoglobin gene). Normalized data were analyzed with GraphPad Prism version 5.

One-way ANOVA with a Tukey's multiple-comparison test was used to assess significant binding of GR and/or MR. Significance was accepted at  $P \leq .05$ .

The primer sequences for ChIP validation are listed in Supplemental Table 1.

### Motif search

The regions containing the GBS were trimmed to 200-bp sequences and screened for de novo motifs consisting of 8 to 40 nucleotides using MEME (multiple expectation maximization for motif elicitation) (38). The 15 most significant motifs were given as output and compared against databases of known motifs using TOMTOM Motif Comparison Tool (39).

### Gene ontology analysis

The genes nearest to the significant GBS were clustered with the Database for Annotation, Visualization, and Integrated Discovery (DAVID) version 6.7 (<http://david.abcc.ncifcrf.gov/home.jsp>) according to their functional annotation.

## Results

### ChIP-Seq results

Sequencing of the DNA fragments acquired by ChIP resulted in the generation of  $1.9 \times 10^7$  and  $1.5 \times 10^7$  reads that were bound by GR and IgG, respectively. Approximately  $1.1 \times 10^6$  and  $0.47 \times 10^6$  reads could be uniquely mapped to the rat genome (rn4) for GR and IgG, respectively. MACS peak calling resulted in the identification of

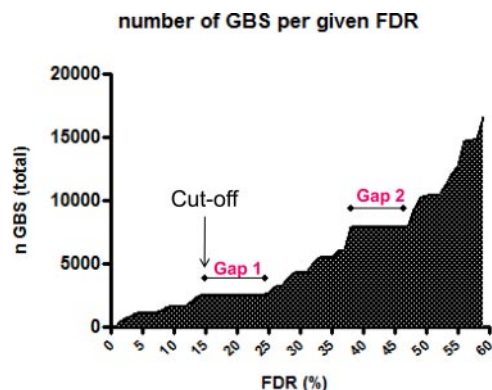


**Figure 1.** The number of GBSs (y-axis) are plotted against the corresponding FDR (x-axis). Two FDR gaps are evident: 1) from 12.98% to 24.08% and 2) from 37.16% to 47.28%, in which a rise in FDR does not yield an increase in GBS. FDRs are shown in percentages.

16 614 peaks that were bound by GR (GBS) with FDR percentages that ranged from 0 to 58 (Supplemental Table 2). Plotting the distribution of FDR values for all GBS revealed that the FDRs were not distributed as a continuum but that there were some gaps in which a range of FDR values were not represented. Based on this, an FDR cutoff of 13% was chosen, which coincided with the point in the FDR distribution curve just before the first major gap (Figure 1). This cutoff resulted in a total of 2460 GBS with  $P$  values ranging from  $3.3 \times 10^{-116}$  to  $1.13 \times 10^{-12}$  (Supplemental Table 3).

### Genomic distribution of GBS in rat hippocampus

The 2460 significant GBS were associated with 1823 unique gene IDs. Examination of the location of the 2460

GBS relative to nearby genes revealed that 965 GBS (39%) were located within genes (Figure 2). Interestingly, the intragenic GBS were mainly located within intronic regions (78%), followed by 5'-untranslated region (UTR) (15%), intron/exon junctions (4%), and 3'-UTR (3%). Only 1% of the intragenic GBS were located within exons. Considering GBS that were located outside annotated RefSeq genes, 12% of GBS were located within 10 kilobases (kb) upstream or downstream from the nearest gene and another 27% between 10 and 100 kb. The remaining 22% were located further than 100 kb upstream or downstream of the nearest genes, of which 111 GBS (5%) were at more than 500 kb.

### Validation of GBS confirms ChIP-Seq results

To validate the results obtained from ChIP-Seq, a selection of 13 GBS covering a wide spectrum of  $P$  values was measured in ChIP samples obtained from an independent set of hippocampi. In all cases, significant GR binding relative to untreated ADX animals was confirmed (Figure 3). Interestingly, there was a large variation in degree of GR binding to the GBS, ranging from 0.06% to 3.5% of the DNA that was bound by GR in the selected genomic regions. In general, the GBS with the highest degree of GR binding were the most significant, with lower FDR and  $P$  values in comparison with GBS with lower levels of GR binding (Figure 3).

### GRs bind to their genomic targets in a ligand concentration-dependent manner

To investigate whether GR binding to its genomic targets was dependent on the concentration of available li-

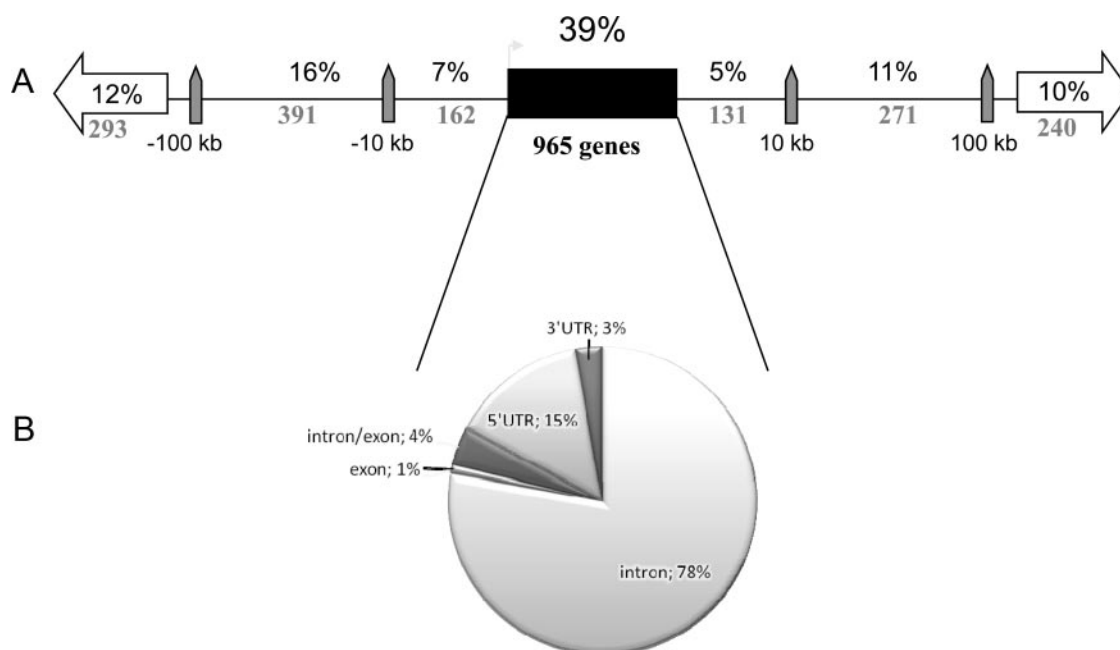


**Figure 2.** A, Distribution of GBS relative to the nearest gene, resulting in regions that lie within or outside genes. The black bar represents a gene, showing that 39% of the GBS are located within genes. The GBS that are located up or downstream from the nearest gene are divided into 3 bins: within 10 kb, between 10 and 100 kb, and more than 100 kb from a gene. B, Pie chart showing the location of intragenic GBS within annotated RefSeq genes, divided into 5'-UTR (exon or intron), intron, exon, intron/exon overlap, and 3'-UTR (exon or intron) regions.



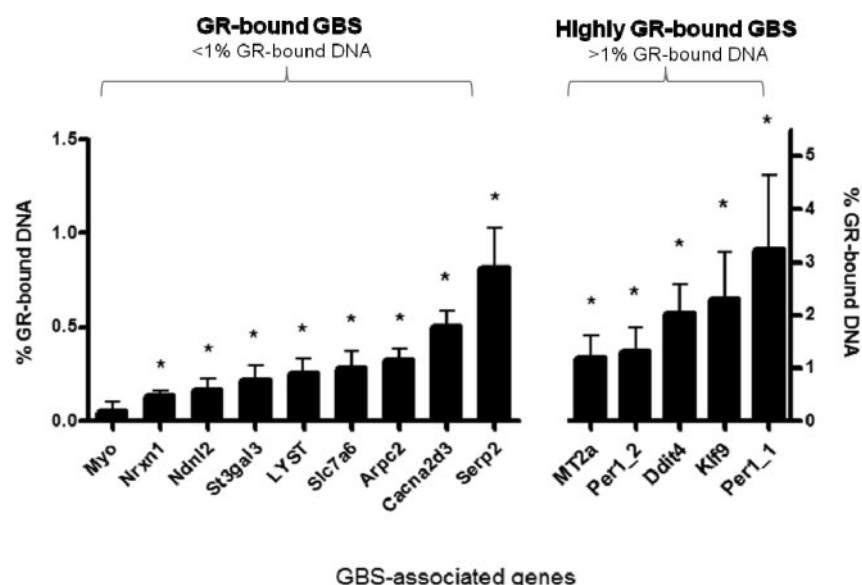


**Figure 3.** Graph showing ChIP-PCR validation of a selection of GBS that were identified by ChIP-Seq. Because the intensity of GR binding varies enormously, the graph was split in two, showing the GBS with lower GR binding on the left (percent GR-bound DNA < 1.0) and GBS with higher GR-binding (percent GR-bound DNA > 1.0) on the right with different y-axes. The gene nearest to the GBS is listed on the x-axis and the percentage of GR-bound DNA (corrected for IgG) is indicated on the y-axis. Statistical analysis was performed using 1-way ANOVA with Tukey's multiple-comparison test to identify GBS that show significant GR binding compared with noninjected animals. \*, Significance was accepted at  $P < .05$ . GR binding in myoglobin exon2 was measured as a negative control. Details of all the validated GBS are present in Supplemental Table 3 (GBS number): *Nr1h1* (1826), *Ndnf2* (1529), *Slc7a6* (529), *Lyst* (535), *Slc7a6* (640), *Arpc2* (759), *Cacna2d3* (1540), *Serp2* (61), *MT2a* (63), *Per1\_2* (1362), *Ddit4* (211), *Klf9* (25), *Per1\_1* (12).

gand, we analyzed GR binding within the hippocampi of 4 groups of animals that received different doses of CORT, namely 3, 30, 300, or 3000  $\mu\text{g}/\text{kg}$ . We performed ChIP-PCR on the same selection of GBS described above (Figure 3). In all cases, significant GR binding was observed in a dose-dependent manner. A more detailed analysis allowed the GBS to be divided into 2 distinct groups based on their differential binding at lower CORT concentrations (Figure 4). The first group, the high-CORT GBS, showed no binding after injecting 3 or 30  $\mu\text{g}/\text{kg}$  CORT, in some cases minimal binding at 300  $\mu\text{g}/\text{kg}$  CORT, but a sharp increase in binding at 3000  $\mu\text{g}/\text{kg}$  CORT (Figure 4A). The second group, the low-CORT GBS, displayed GR binding starting at 30  $\mu\text{g}/\text{kg}$  CORT, which increased thereafter and reached relatively high levels of GR binding at the highest CORT concentration of 3000  $\mu\text{g}/\text{kg}$  (Figure 4C). Interestingly, the low-CORT group coincided with the most intensely bound GBS and the high-CORT group with the less intensely bound GBS (Figure 3).

### MRs and GRs bind to the same GBSs, but at different ratios depending on the ligand concentration

Although the binding sites reported here were identified using a GR-specific antibody, we were interested in

whether they might also be bound by MR, because MR and GR have DNA-binding domains that are 94% identical and may form heterodimers. Because MR and GR have different affinities for CORT, we performed ChIP for MR and GR under varying amounts of available ligand, ranging from 3 to 3000  $\mu\text{g}/\text{kg}$ . The lowest dose of 3  $\mu\text{g}/\text{kg}$  was chosen, because we expected both poor activation of GR and MR and hence very little DNA binding to be observed at this CORT concentration. The next dose of 30  $\mu\text{g}/\text{kg}$  was chosen because we expected predominant MR activation and very little GR activation, whereas 300 and 3000  $\mu\text{g}/\text{kg}$  are in the CORT range of additional significant GR activation. Significant MR binding was observed at all GBS except at *Per1\_2*, *MT2a*, and *Slc7a6*. Analysis of MR binding to the low-CORT and high-CORT GBS described above showed a different binding pattern than GR binding (Figure 4, B and D), with MR binding starting at either 30 or

300  $\mu\text{g}/\text{kg}$  CORT but not increasing at higher CORT doses. This is in contrast to GR binding, where a sharp increase at 3000  $\mu\text{g}/\text{kg}$  CORT was observed. Calculating the ratio of MR and GR binding to the validated GBS showed that the low-CORT GBS have a GR to MR ratio above 1, indicating that they display relatively more GR binding over the full range of CORT concentrations ranging from 30 to 3000  $\mu\text{g}/\text{kg}$ . In contrast, the high-CORT GBS mostly have a GR to MR binding ratio below 1, in particular in the CORT concentration range of 3 to 300  $\mu\text{g}/\text{kg}$ .

### Motif analysis reveals Zbtb3 to be an important possible transactivation partner

A remarkably high proportion of GBS contained a GRE. The GRE sequence itself was identical to the consensus sequence that was identified in other ChIP-Seq studies on GR (Figure 5) (21–23).

Only 14 of the 2460 GBS lacked a GRE, indicating that the remaining 2446 GBS likely regulate target gene expression through direct GR-GRE interaction, also known as transactivation. Continuing the motif screening within the 500 GRE-containing GBS with the lowest FDR revealed that 288 GBS (58%), in addition to a GRE motif,

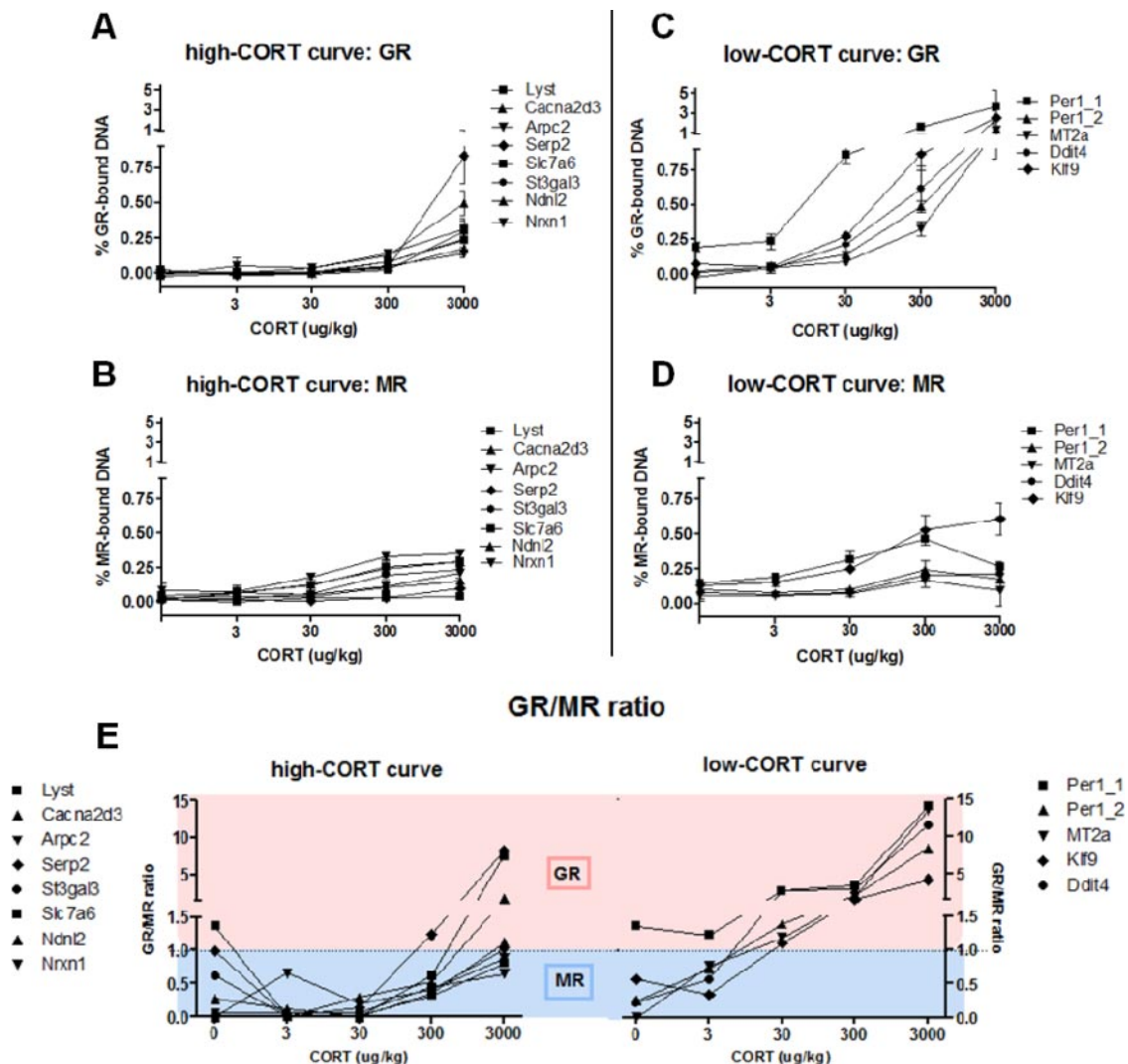


**Figure 4.** Graphs visualizing the concentration-dependent binding of GR and MR to its targets. The CORT concentration is indicated on the x-axis. Point 0 of the x-axis represents undisturbed animals that did not receive a CORT injection. The GBS were assigned into 2 different groups: the high-CORT and the low-CORT groups. A, GR binding to the high-CORT group is shown, in which GR binding to the GBS is evident after injecting 3000  $\mu\text{g/kg}$  but not at lower concentrations. B, MR binding to these high-CORT GBS is apparent at 30  $\mu\text{g/kg}$  as well but in most cases stabilizes thereafter. C, GR binding to low-CORT GBS, where GR binding is present at 30  $\mu\text{g/kg}$  CORT and increases with higher CORT concentrations. D, MR binding to low-CORT GBS that resembles the pattern observed in the high-CORT GBS. E, Graph in which the GR to MR ratio for the high-CORT and low-CORT groups are visualized. All GBS were significantly bound by GR according to 1-way ANOVA analysis with Tukey's multiple-comparison test relative to noninjected animals. Significance was accepted at  $P < .05$ .

also contained a motif that significantly resembled the binding motif of the transcription factor zinc finger and BTB domain containing 3 (Zbtb3) (Figure 5). Other identified motifs involved sequences similar to binding sites for zinc finger protein 740 (Zfp740), SRY-box containing gene 12 (Sox12), Sox4, serum response factor (Srf), and zinc finger and SCAN domain containing 4C (GM397 or Zscan4c). Analysis of the top 5 co-occurring motifs within 1 GBS revealed that the combination of GR and Zbtb3 binding motifs within the GBS without the presence of any of the other motifs was most prevalent (37%) (Figure 6). This was followed by the combination of GR, Zbtb3, and zinc finger protein 740

or Sox12 binding motifs, both combinations occurring in 10% of this selection of GRE-containing GBS. Co-occurrence of GR with Sox12 or Sox4 binding motifs was observed in 7% of these GBS.

Of the 14 GBS that did not contain a GRE, all contained 2 motifs significantly resembling the motif recognized by the protein CG11181 gene product from transcript CG11181-RB (CUP) (Figure 5). Eight of these GBS (57%) additionally contained a binding motif significant for the zinc-coordinating protein zf-C2H2 Zinc finger, C2H2 type (RME1). Binding motifs resembling the transcription factor specificity protein 1 and interferon regulatory factor 2 (Irf2) binding sites occurred in 6 GBS (43%) (Figure 6).

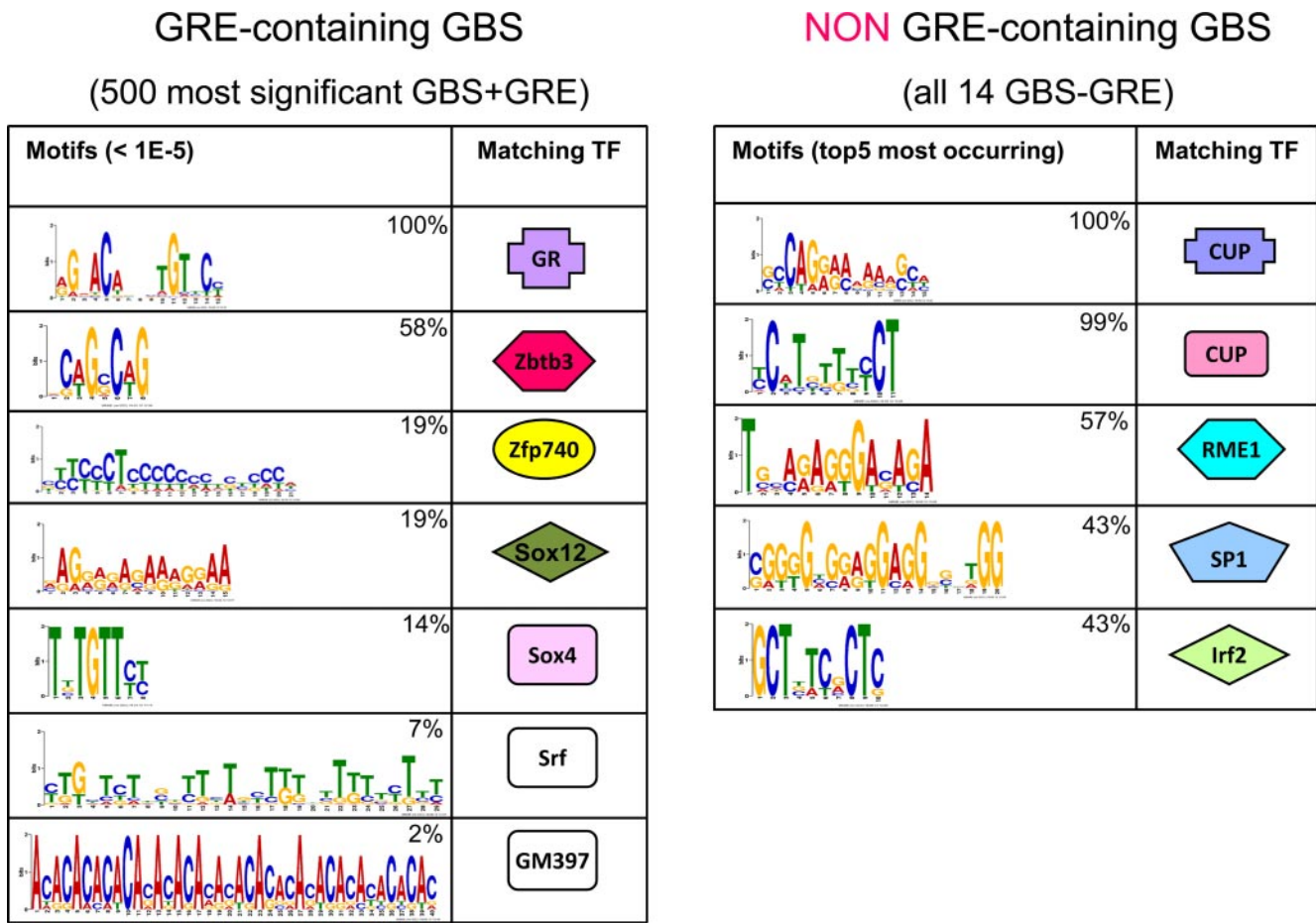


**Figure 5.** Motifs identified in GBS that do or do not contain a GRE. For GBS that do contain a GRE, the motifs with an e-value < 0.05 were considered. Because only 14 GBS did not contain a GRE, all e-values are higher than 0.05 and therefore the 5 most frequent occurring motifs are depicted. The e-value indicates the statistical significance of the motif and is calculated by MEME. The e-value is an estimate of the expected number of motifs with the given log likelihood ratio (or higher), and with the same width and site count, that one would find in a similarly sized set of random sequences.

**GBS-associated genes are involved in neuronal functioning and cell survival**

To investigate the biological relevance of the identified GBS, we analyzed the functional annotations of the 2460

associated genes and sorted them into clusters using DAVID (Table 2). Within the top 10 clusters, we found neuronal-associated clusters, namely, cell and neurite projection (cluster 1) and neuron differentiation (cluster 9) as well as cell-survival clusters like apoptosis (cluster 5) and regulation of programmed cell death (cluster 7). The remaining clusters involved enzyme binding (cluster 3), response to organic substance (cluster 4), phosphate metabolic process (cluster 8), and positive regulation of transcription (cluster 10).

As described above, a motif resembling Zbtb3-binding sequences was identified in 58% of the 500 GRE-containing GBS that have the lowest FDR. We next investigated whether the genes associated with these Zbtb3-containing GBS were involved in different biological pro-

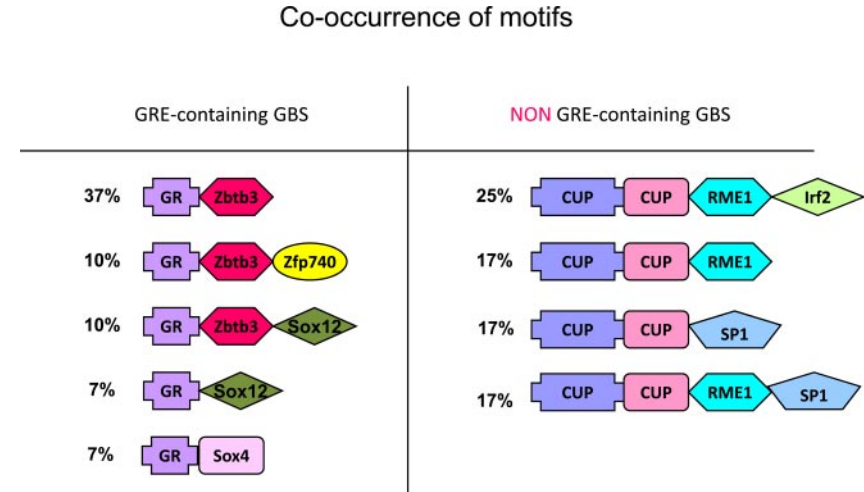


**Figure 6.** Most frequently observed combinations of motifs identified within GBS with or without a GRE. For GBS that did contain a GRE, the top 5 co-occurring motifs are depicted. For GBS without a GRE, all observed combinations are shown.



**Table 2.** Top 10 Enriched Functional GO Clusters of GBS-Associated Genes Identified in Rat Hippocampus

	GO Term	Category	ES
1	Cell and neurite projection	CC	6.8
2	Blood vessel development	BP	6.3
3	Enzyme binding	MF	5.5
4	Response to organic substance	BP	5.4
5	Apoptosis	BP	5.2
6	Cell and membrane fraction	CC	5.0
7	Regulation of programmed cell death	BP	4.3
8	Phosphate metabolic process	BP	4.0
9	Neuron differentiation	BP	4.0
10	Positive regulation of transcription	BP	3.9

The 10 most enriched functional GO clusters in GBS-associated genes in rat hippocampus. Analysis was performed with DAVID under medium classification stringency. Per cluster, the first GO term is shown. In addition, the category to which the GO term belongs to is indicated: biological processes (BP), molecular function (MF), or cellular compartment (CC). The enrichment score (ES) indicates the geometric mean (in  $-\log$  scale) of the cluster member's *P* value.

cesses and functions from the GBS without a *Zbtb3*-binding sequence. Clustering of the acquired gene ontology (GO) revealed differences between GBS that do or do not contain a *Zbtb3*-binding sequence with regard to the types of clusters and the degree of enrichment (Table 3). GBS harboring a *Zbtb3* motif generally had clusters with higher enrichment scores compared with GBS without *Zbtb3* motifs. For example, 7 clusters showed an enrichment of more than 2 versus only 2 clusters with this degree of enrichment in the group lacking a *Zbtb3* motif. Furthermore, the *Zbtb3*-containing group was enriched for clusters involved in regulation of apoptosis (clusters 4 and 5), regulation of transcription (cluster 3), and regulation of macromolecule metabolic process and insulin receptor

signaling pathway (cluster 6 and 7). The non-*Zbtb3*-containing group, in contrast, was mainly involved in protein kinase binding (cluster 1, 3.7 enrichment), followed by ion binding and biological adhesion.

## Discussion

Because neuronal plasticity within the hippocampus is known to be very sensitive to GR activation, resulting in functional as well as structural changes (19, 40, 41), we were interested in the composition of the GR-binding repertoire within hippocampal tissue. In the current study in rat hippocampus, we identified 2460 significant GBS using ChIP-Seq. Analysis of a selection of these GBS in animals that received different doses of CORT showed that the GR-binding potential differs depending on the GBS that is analyzed and the concentration of ligand that has been administered. We showed MR binding to several validated GBS, but to a lower extent than GR binding, in particular at the higher CORT concentrations. Finally, motif analysis revealed a high prevalence of sequences within the GBS that significantly resemble binding sites for *Zbtb3* and CUP, which might be potential new cross-talk partners involved in GR-mediated transactivation and transrepression, respectively.

## Reliability of ChIP-Seq data

To validate the reliability of our GBS, we randomly selected 13 GBS with FDRs ranging from 0% to 13% for validation by ChIP-PCR. In all cases, we were able to suc-

**Table 3.** Top 10 Enriched Functional GO Clusters in Rat Hippocampus in the 500 Most Significant GBS-Associated Genes With and Without *Zbtb3* Motifs

With <i>Zbtb3</i>				Without <i>Zbtb3</i>		
	GO Term	Category	ES		Category	ES
1	Negative regulation of cell communication	BP	3.9	Protein kinase binding	MF	3.7
2	Insoluble fraction	CC	3.0	Ion binding	MF	2.3
3	Negative regulation of transcription	BP	2.7	Biological adhesion	BP	1.9
4	Regulation of apoptosis	BP	2.7	Protein amino acid dephosphorylation	BP	1.3
5	Positive regulation of anti-apoptosis	BP	2.5	Eye morphogenesis	BP	1.3
6	Positive regulation of macromolecule metabolic process	BP	2.4	Protein kinase cascade	BP	1.3
7	Negative regulation of insulin receptor signaling pathway	BP	2.3	In utero embryonic development	BP	1.2
8	Blood vessel development	BP	1.7	Regulation of nucleotide biosynthetic process	BP	1.1
9	Regulation of cell-substrate adhesion	BP	1.7	Mitochondrial part	CC	1.0
10	Response to inorganic substance	BP	1.6	Rhythmic process	BP	1.0

The 10 most enriched functional GO clusters in associated genes that are found in GBS with GRE and *Zbtb3* motifs (left columns) or GBS containing only a GRE motif and lacking a *Zbtb3* motif (right columns). Analysis was performed with DAVID. Per cluster, the first GO term is shown. In addition, the category to which the GO term belongs to is indicated: biological processes (BP), molecular function (MF), or cellular compartment (CC). The enrichment score (ES) indicates the geometric mean (in  $-\log$  scale) of the clusters member's *P* values.



cessfully validate GR binding to the GBS, supporting that the statistical threshold we applied was stringent enough to detect bona fide GBS. The fact that 99% of the GBS that we considered to be significant contain a GRE, in our opinion, strengthens the hypothesis that these are real GBS. In a previous ChIP-Seq study on genome-wide GR binding in neuronal PC12 cells, we observed that more than 80% of the 100 most significant GBS contained a GRE, with this percentage slowly decreasing as GBS significance descended (24), suggesting that our cutoff detecting 2460 GBS may even have been too stringent. GRE-dependent processes are important in the brain, as shown in GR<sup>dim/dim</sup> mutant mice, in which the mutation prevented GR homodimerization and therefore binding to most GREs. These mice showed an impairment of modulation of hippocampal excitability and spatial memory (42, 43).

Additional support for the reliability of the ChIP-Seq data presented here comes from the observation of hippocampal GR binding near several known GR targets such as *Per1*, *Ddit4* (24, 44, 45), *Mt2a*, and *Klf9* (24, 44, 45) as well as near many genes previously reported to be differentially regulated upon a psychological or physiological stressor, such as, microtubule-associated protein 2 (*MAP2*) (46), microtubule-associated protein 1b (*MAP1b*) (47), neuroligin 1 (*nlgn1*) (48), growth-associated protein 43 (*GAP43*) (49), calcium/calmodulin-dependent protein kinase II $\alpha$  (*Camk2a*) (50), FK506 binding protein (*Fkbp5*) (51), glutamate receptor, ionotropic, N-methyl D-aspartate 2B (*Grin2b*) (52), glutamate receptor, ionotropic, AMPA 2 (*Gria2*) (53), and N-myc downregulated gene 2 (*NDRG2*) (54). Interestingly, *NDRG2* is a target of MR and is activated by the MR ligand aldosterone in the kidney and distal colon (55).

The GR-binding data were obtained in ADX rats replaced with a specific dose of CORT, which creates an artificial context due to the depletion of endogenous CORT. However, the fact that we detected several known GR targets and almost all binding sites contained a highly significant GRE sequence does give us confidence in the data.

### A high percentage of GBSs are located within introns or far away from genes

A relatively high percentage (39%) of the 2460 significant GBS was located within genes, in particular within introns, which is a finding that we previously observed in neuronal PC12 cells and that has also been observed by others (22–24). It is becoming increasingly clear that many intronic regions have a regulatory function and harbor *cis*-acting regulatory elements such as tissue-specific enhancers (56–59) and noncoding RNAs, which play an

important role in autoregulation and gene regulation processes (60, 61). Approximately 22% of the GBS were located at distances of at least 100 kb from the nearest gene and 5% at even 500 kb or more. It has been shown that these gene deserts that are devoid of coding sequence may contain regulatory sequences that act at large distances to control gene expression (62).

### GR binding to genomic targets is dependent on ligand availability

A few studies have shown dose-response effects of CORT on the expression of target genes (63, 64). We studied the dose-response relationship of GR binding to a selection of the GBS identified after administration of a high dose of CORT (3000  $\mu$ g/kg). Our results indicated that in a subset of GBS, the high-CORT GBS, GR binding to the GBS became evident only after injecting 3000  $\mu$ g/kg CORT, but not at lower CORT concentrations. In contrast, another subset had a more step-wise GR-binding profile, starting at 30  $\mu$ g/kg CORT and slowly increasing thereafter, which we called the low-CORT GBS. Interestingly, the low-CORT GBS had the lowest FDRs and the highest relative GR binding (Figure 4). Hence, these low-CORT GBS represent the binding sites that become occupied upon replacement of the ADX animal with CORT toward physiological levels, whereas the high-CORT group is identified in a dose range common for pharmacotherapy of inflammatory processes, a distinction that has been indicated by Sapolsky et al (65) as indicative for permissive and regulatory (eg, stimulatory, suppressive, and preparative) actions of GCs.

What could the differences in GR-binding potential to the various targets implicate? First, it appears that the GC concentration affects the repertoire of genomic targets to which GRs bind. The GBS near the low-CORT genes are bound at relatively low levels of CORT as well as at higher levels of CORT. This indicates that these genes are likely to be activated during daily variations of CORT. The high-CORT GBS, conversely, appear to be less sensitive to changing CORT levels. Only when the organism is exposed to a higher concentration of CORT, which may occur at the circadian peak or in response to more severe stressors, and the concentration of the hormone is sufficiently high for the activation of GR will binding of GR to these high-CORT GBS occur, resulting in the activation of the corresponding genes near these GBS. The question can therefore be raised, whether the distinction in low-CORT and high-CORT genes may relate to the enormous diversity in permissive and regulatory actions of GCs that have been suggested to be complementary in coordination of daily activities and sleep-related events as well as organization of the response to stress, respectively (65).

Interestingly, classical known GR targets such as *Per1*, *Ddit4*, *Mt2a*, and *Klf9*, ubiquitously bound by GRs in multiple cell types and tissues, were all present within the low-CORT group and perhaps may therefore be important for any kind of daily variation in actions of a permissive nature. Our findings imply that, depending on the amount of secreted CORT, different sets of GR-target genes are recruited in the hippocampus. Because the level of CORT secretion is directly related to duration and severity of the stressor, this may explain how the high-CORT GBS affect the profound functional and structural changes in plasticity of hippocampal neurons caused by chronic GC overexposure.

### MRs bind to GBS, but at lower CORT concentrations

Knowledge of MR targets is sparse, in particular in the brain. Because MR have a near identical DNA-binding domain to GR, we were curious whether MR also displayed binding to GBS. Both receptors are activated by the ligand CORT, with the only difference that MR have a much higher affinity for CORT and, consequently, are activated at lower CORT levels in comparison with GR. In particular in the high-CORT GBS, MR binding at the lower CORT concentrations might disable GR binding and allow GR binding only when CORT levels become so high that MR are fully occupied. Indeed, we observed relatively higher MR binding to the high-CORT GBS than to the low-CORT GBS. At an absolute level, the difference in MR binding was not apparent, indicating a saturation of MR in both situations, further supporting the importance of the balance in MR- and GR-mediated actions in maintaining homeostasis (5).

It is unlikely that the differences in MR and GR binding can be linked to differences in relative concentrations of MR and GR protein levels in the hippocampal preparations we used, although we did not measure this in the current study. However, it is known from our original radioligand binding and Western blot studies over the years that MR and GR concentrations in hippocampus are in the same range but that the values may change depending on strain, age, and stress history. Reul and de Kloet (3) reported an MR concentration of 250 fmol/mg protein in the hippocampus cytosol of ADX Wistar rats, whereas the GR concentration was 310 fmol/mg protein.

GR monomers may also form dimers via heterodimerization with MR, potentially increasing the level of functional diversity (66). A recent study using green fluorescent protein-based fluorescence resonance energy transfer in living cultured hippocampal neurons provided evidence that MR and GR directly interact with each other in the nucleus (67). The results from this study suggested

that MR may predominantly form homodimers at lower CORT concentrations, whereas at higher concentrations mimicking stressful conditions when GR activation becomes more abundant, the incidence of heterodimerization with GR increased (67).

We have previously reported that MR and GR have distinct yet overlapping target genes in the hippocampus (68). Strikingly, MR bound to almost all the GBS we tested here. However, because the study was designed to identify GBS and not MR-binding sites, we cannot exclude the existence of MR-specific binding sites that might be detected in a genome-wide screen using an MR-specific antibody.

### GBS near CORT-regulated genes are involved in neuronal plasticity

Recent insights from ChIP-Seq studies have revealed that GR bind to the genome in a cell-type-specific manner. Therefore we expect GR to target genomic sites in the hippocampus that are different from those in other non-neuronal cell types (21–24). Because GR play an important role in hippocampal neuronal plasticity, we hypothesized that GBS in the hippocampus would be located nearby or within genes associated with neuronal plasticity. Indeed, we observed GR binding near several genes involved in neuronal plasticity, such as neurochondrin (*NCDN*), ionotropic N-methyl-D aspartate (NMDA) receptor-2 (*GRIN2A* and *GRIN2B*), metabotropic 5 (*GRM5*), and signal-induced proliferation-associated 1 like 1 glutamate receptor (*SIPA1L1*). Furthermore, GO analysis showed that GR bind to genomic sites that are located near genes involved in neuron projection and neuron differentiation, which were overrepresented GO terms.

An important pathway that is known to be involved in cell survival and neuronal plasticity is the mammalian target of rapamycin (mTOR) pathway. We have recently shown that a number of regulators of the mTOR pathway, such as *Ddit4* and *Fkbp51* are primary targets of GR and are differentially expressed within the rat hippocampus after a CORT challenge (31). In the current study, we confirmed these primary binding sites and in addition observed GR binding near other mTOR pathway members, such as phosphatidylinositol 3-kinase, catalytic subunit type 3 (*Pik3c3*) and regulatory subunit 1 [alpha] (*Pik3r1*) as well as Pi3k-regulator insulin receptor substrate 2 (*Irs2*). Interestingly, phosphatidylinositol 3-kinase signaling is indicated to play a key role in mediating the stress-induced modification of hippocampal synaptic plasticity (69). Strikingly, brain-specific deletion of the *Irs2* gene is associated with disrupted hippocampal synaptic plasticity (70). These findings support our previous proposal that

direct regulation of the mTOR pathway by CORT represents an important mechanism regulating neuronal plasticity in the rat hippocampus (31).

### Hippocampal GBS provide new insight into cross-talk partners of GR in the brain

The extremely high proportion of GRE-containing GBS (99%) is considerably higher than observed in other GR ChIP-Seq studies, where GRE percentages ranged from 60% to 80% (21–24). However, the present study differs in several aspects from previous ChIP-Seq studies, which were all performed in vitro in cell lines and also used the synthetic ligand dexamethasone instead of the natural GR ligand CORT. Different GR ligands are known to differentially affect the conformation state of GR, with consequences for the availability of the ligand-binding domain of GR, dissociation rate from the DNA, and its affinity to interact with the genome (71).

GR regulate gene transcription in conjunction with an extensive network of other transcription factors. Almost 60% of the GBS consisted of composite sites containing a motif for Zbtb3 besides a GRE. Zbtb3 was identified as a potential interaction partner of GR (72). Interestingly, we previously identified a motif for Zbtb3 to be present in 81% of the GBS that lacked a GRE in neuronal PC12 cells (24). Together these findings suggest that Zbtb3 may play a role in directing GR to their binding sites within the hippocampus. Unfortunately, not much is known about this protein, and its precise role in GR signaling requires further exploration.

The 14 GBS that did not contain a GRE all contained motifs for the DNA-binding sequence of CUP, a protein that has been studied extensively in *Drosophila* but not at all in mammals yet (73). CUP is an eukaryotic translation initiation factor 4E (EIF4E)-binding protein that represses the expression of specific maternal mRNAs. Interestingly, eukaryotic translation initiation factor 4E (EIF4E)-binding protein is an upstream component of the mTOR pathway, which we have previously identified to be regulated by GR within the brain. CUP may therefore be an interesting potential novel cross-talk partner of GR in the hippocampus.

A striking observation in this study is the complete lack of binding sites for classical GR cross-talk partners like activation protein-1 (74) and nuclear factor- $\kappa$ B (75), which are known to occur both in composite sites together with a GRE as well as in sites lacking a GRE. Similar to our previous study on GR binding in neuronal PC12 cells, we identified motifs for transcription factors that had not previously been associated with GR function within the GBS (24). A likely explanation for this is that most of the cross-talk partners of GR were identified in studies on the im-

munosuppressive and tumor-suppressive properties of GR (75–77), whereas until now, very little effort has been put into identifying cross-talk partners in a neuronal context.

In conclusion, the current study has provided new insight into GR functioning in the brain. Besides having identified thousands of genomic GBS within the hippocampus, we have shown that under varying GC concentrations, different binding sites are recruited. Our results highlight the existence of 2 distinct populations of GBS in the rat hippocampal genome that can be discriminated by the extent of CORT binding. Furthermore, within the GBS, we have identified several motifs for proteins that may be potential cross-talk partners of GR within the hippocampal interactome.

### Acknowledgments

We thank Nagesha Rao and Robert de Jonge for their assistance in the bioinformatics analysis.

Address all correspondence and requests for reprints to: Dr N. A. Datson, Prosensa Therapeutics, PO Box 281, 2300 AG Leiden, The Netherlands. E-mail: n.datson@prosenza.nl.

This work was supported by grants from the Netherlands Organization for Scientific Research (NWO) 836.06.010 (MEER Vrouwelijke Onderzoekers als UD, MEERVOUD) to N.A.D., Top Institute (TI) Pharma T5-209, and Human Frontiers of Science Program (HFSP) (RGP39). E.R.d.K. was supported by the Royal Netherlands Academy of Science.

Disclosure Summary: The authors have nothing to disclose.

### References

1. Chao HM, Choo PH, McEwen BS. Glucocorticoid and mineralocorticoid receptor mRNA expression in rat brain. *Neuroendocrinology*. 1989;50:365–371.
2. Morimoto M, Morita N, Ozawa H, Yokoyama K, Kawata M. Distribution of glucocorticoid receptor immunoreactivity and mRNA in the rat brain: an immunohistochemical and in situ hybridization study. *Neurosci Res*. 1996;26:235–269.
3. Reul JM, de Kloet ER. Two receptor systems for corticosterone in rat brain: microdistribution and differential occupation. *Endocrinology*. 1985;117:2505–2511.
4. de Kloet ER, Joels M, Holsboer F. Stress and the brain: from adaptation to disease. *Nat Rev Neurosci*. 2005;6:463–475.
5. de Kloet ER, Vreugdenhil E, Oitzl MS, Joels M. Brain corticosteroid receptor balance in health and disease. *Endocr Rev*. 1998;19:269–301.
6. Chandler VL, Maler BA, Yamamoto KR. DNA sequences bound specifically by glucocorticoid receptor in vitro render a heterologous promoter hormone responsive in vivo. *Cell*. 1983;33:489–499.
7. Bruna A, Nicolas M, Munoz A, Kyriakis JM, Caelles C. Glucocorticoid receptor-JNK interaction mediates inhibition of the JNK pathway by glucocorticoids. *EMBO J*. 2003;22:6035–6044.
8. Herrlich P, Ponta H. Mutual cross-modulation of steroid/retinoic acid receptor and AP-1 transcription factor activities: a novel prop-



- erty with practical implications. *Trends Endocrinol Metab.* 1994; 5:341–346.
9. Scheinman RI, Gualberto A, Jewell CM, Cidlowski JA, Baldwin AS Jr. Characterization of mechanisms involved in transrepression of NF- $\kappa$ B by activated glucocorticoid receptors. *Mol Cell Biol.* 1995; 15:943–953.
  10. van Steensel B., van Binnendijk EP, Hornsby CD, van der Voort HT, Krozowski ZS, de Kloet ER, van Driel R. Partial colocalization of glucocorticoid and mineralocorticoid receptors in discrete compartments in nuclei of rat hippocampus neurons. *J Cell Sci.* 1996;109(Pt 4):787–792.
  11. Chen Y, Dube CM, Rice CJ, Baram TZ. Rapid loss of dendritic spines after stress involves derangement of spine dynamics by corticotropin-releasing hormone. *J Neurosci.* 2008;28:2903–2911.
  12. Shors TJ, Chua C, Falduto J. Sex differences and opposite effects of stress on dendritic spine density in the male versus female hippocampus. *J Neurosci.* 2001;21:6292–6297.
  13. Alfarez DN, Joels M, Krugers HJ. Chronic unpredictable stress impairs long-term potentiation in rat hippocampal CA1 area and dentate gyrus in vitro. *Eur J Neurosci.* 2003;17:1928–1934.
  14. Bodnoff SR, Humphreys AG, Lehman JC, Diamond DM, Rose GM, Meaney MJ. Enduring effects of chronic corticosterone treatment on spatial learning, synaptic plasticity, and hippocampal neuropathology in young and mid-aged rats. *J Neurosci.* 1995;15:61–69.
  15. Krugers HJ, Goltstein PM, van der Linden S, Joels M. Blockade of glucocorticoid receptors rapidly restores hippocampal CA1 synaptic plasticity after exposure to chronic stress. *Eur J Neurosci.* 2006; 23:3051–3055.
  16. Datson NA, Morsink MC, Meijer OC, de Kloet ER. Central corticosteroid actions: search for gene targets. *Eur J Pharmacol.* 2008; 583:272–289.
  17. Morsink MC, Steenbergen PJ, Vos JB, et al. Acute activation of hippocampal glucocorticoid receptors results in different waves of gene expression throughout time. *J Neuroendocrinol.* 2006;18: 239–252.
  18. Andrus BM, Blizinsky K, Vedell PT, et al. Gene expression patterns in the hippocampus and amygdala of endogenous depression and chronic stress models. *Mol Psychiatry.* 2012;17:49–61.
  19. Datson NA, Speksnijder N, Mayer JL, et al. The transcriptional response to chronic stress and glucocorticoid receptor blockade in the hippocampal dentate gyrus. *Hippocampus.* 2012;22:359–371.
  20. Lisowski P, Juszczak GR, Goscik J, Wiczorek M, Zwierzchowski L, Swiergiel AH. Effect of chronic mild stress on hippocampal transcriptome in mice selected for high and low stress-induced analgesia and displaying different emotional behaviors. *Eur Neuropsychopharmacol.* 2011;21:45–62.
  21. John S, Sabo PJ, Thurman RE, et al. Chromatin accessibility pre-determines glucocorticoid receptor binding patterns. *Nat Genet.* 2011;43:264–268.
  22. Reddy TE, Pauli F, Sprouse RO, et al. Genomic determination of the glucocorticoid response reveals unexpected mechanisms of gene regulation. *Genome Res.* 2009;19:2163–2171.
  23. Yu CY, Mayba O, Lee JV, et al. Genome-wide analysis of glucocorticoid receptor binding regions in adipocytes reveal gene network involved in triglyceride homeostasis. *PLoS One.* 2010;5:e15188.
  24. Polman JA, Welten JE, Bosch DS, et al. A genome-wide signature of glucocorticoid receptor binding in neuronal PC12 cells. *BMC Neurosci.* 2012;13:118.
  25. Sarabdjitsingh RA, Isenia S, Polman A, et al. Disrupted corticosterone pulsatile patterns attenuate responsiveness to glucocorticoid signaling in rat brain. *Endocrinology.* 2010;151:1177–1186.
  26. Sarabdjitsingh RA, Meijer OC, de Kloet ER. Specificity of glucocorticoid receptor primary antibodies for analysis of receptor localization patterns in cultured cells and rat hippocampus. *Brain Res.* 2010;1331:1–11.
  27. Champagne DL, Bagot RC, van Hasselt F, et al. Maternal care and hippocampal plasticity: evidence for experience-dependent structural plasticity, altered synaptic functioning, and differential responsiveness to glucocorticoids and stress. *J Neurosci.* 2008;28:6037–6045.
  28. van der Laan S, Sarabdjitsingh RA, Van Batenburg MF, et al. Chromatin immunoprecipitation scanning identifies glucocorticoid receptor binding regions in the proximal promoter of a ubiquitously expressed glucocorticoid target gene in brain. *J Neurochem.* 2008; 106:2515–2523.
  29. Chan O, Inouye K, Akirav EM, et al. Hyperglycemia does not increase basal hypothalamo-pituitary-adrenal activity in diabetes but it does impair the HPA response to insulin-induced hypoglycemia. *Am J Physiol Regul Integr Comp Physiol.* 2005;289:R235–R246.
  30. Owen D, Matthews SG. Glucocorticoids and sex-dependent development of brain glucocorticoid and mineralocorticoid receptors. *Endocrinology.* 2003;144:2775–2784.
  31. Polman JA, Hunter RG, Speksnijder N, et al. Glucocorticoids modulate the mTOR pathway in the hippocampus: differential effects depending on stress history. *Endocrinology.* 2012;153:4317–4327.
  32. Li H, Durbin R. Fast and accurate short read alignment with Burrows-Wheeler transform. *Bioinformatics.* 2009;25:1754–1760.
  33. Quinlan AR, Hall IM. BEDTools: a flexible suite of utilities for comparing genomic features. *Bioinformatics.* 2010;26:841–842.
  34. Zhang Y, Liu T, Meyer CA, et al. Model-based analysis of ChIP-Seq (MACS). *Genome Biol.* 2008;9:R137.
  35. Blankenberg D, Von KG, Coraor N, et al. Galaxy: a web-based genome analysis tool for experimentalists. *Curr Protoc Mol Biol.* 2010;Chapter 19:Unit 19.10.1–21.
  36. Goecks J, Nekrutenko A, Taylor J. Galaxy: a comprehensive approach for supporting accessible, reproducible, and transparent computational research in the life sciences. *Genome Biol.* 2010;11: R86.
  37. Kelly EJ, Sandgren EP, Brinster RL, Palmiter RD. A pair of adjacent glucocorticoid response elements regulate expression of two mouse metallothionein genes. *Proc Natl Acad Sci U S A.* 1997;94:10045–10050.
  38. Bailey TL, Elkan C. Fitting a mixture model by expectation maximization to discover motifs in biopolymers. *Proc Int Conf Intell Syst Mol Biol.* 1994;2:28–36.
  39. Gupta S, Stamatoyannopoulos JA, Bailey TL, Noble WS. Quantifying similarity between motifs. *Genome Biol.* 2007;8:R24.
  40. McLaughlin KJ, Gomez JL, Baran SE, Conrad CD. The effects of chronic stress on hippocampal morphology and function: an evaluation of chronic restraint paradigms. *Brain Res.* 2007;1161:56–64.
  41. Sousa N, Lukoyanov NV, Madeira MD, Almeida OF, Paula-Barbosa MM. Reorganization of the morphology of hippocampal neurites and synapses after stress-induced damage correlates with behavioral improvement. *Neuroscience.* 2000;97:253–266.
  42. Karst H, Karten YJ, Reichardt HM, de Kloet ER, Schutz G, Joels M. Corticosteroid actions in hippocampus require DNA binding of glucocorticoid receptor homodimers. *Nat Neurosci.* 2000;3:977–978.
  43. Oitzl MS, Reichardt HM, Joels M, de Kloet ER. Point mutation in the mouse glucocorticoid receptor preventing DNA binding impairs spatial memory. *Proc Natl Acad Sci U S A.* 2001;98:12790–12795.
  44. Datson NA, Polman JA, de Jonge RT, et al. Specific regulatory motifs predict glucocorticoid responsiveness of hippocampal gene expression. *Endocrinology.* 2011;152:3749–3757.
  45. So AY, Chaivorapol C, Bolton EC, Li H, Yamamoto KR. Determinants of cell- and gene-specific transcriptional regulation by the glucocorticoid receptor. *PLoS Genet.* 2007;3:e94.
  46. Cereseto M, Reines A, Ferrero A, Sifonios L, Rubio M, Wikinski S. Chronic treatment with high doses of corticosterone decreases cytoskeletal proteins in the rat hippocampus. *Eur J Neurosci.* 2006; 24:3354–3364.
  47. Antonow-Schlorke I, Schwab M, Li C, Nathanielsz PW. Glucocorticoid exposure at the dose used clinically alters cytoskeletal proteins



- and presynaptic terminals in the fetal baboon brain. *J Physiol*. 2003; 547:117–123.
48. Dai J, Wang X, Chen Y, Wang X, Zhu J, Lu L. Expression quantitative trait loci and genetic regulatory network analysis reveals that *Gabra2* is involved in stress responses in the mouse. *Stress*. 2009; 12:499–506.
  49. Pascale A, Amadio M, Caffino L, Racagni G, Govoni S, Fumagalli F. ELAV-GAP43 pathway activation following combined exposure to cocaine and stress. *Psychopharmacology (Berl)*. 2011;218:249–256.
  50. Orsetti M, Di Brisco F, Canonico PL, Genazzani AA, Ghi P. Gene regulation in the frontal cortex of rats exposed to the chronic mild stress paradigm, an animal model of human depression. *Eur J Neurosci*. 2008;27:2156–2164.
  51. Lee RS, Tamashiro KL, Yang X, et al. Chronic corticosterone exposure increases expression and decreases deoxyribonucleic acid methylation of *Fkbp5* in mice. *Endocrinology*. 2010;151:4332–4343.
  52. Ayalew M, Le-Niculescu H, Levey DF, et al. Convergent functional genomics of schizophrenia: from comprehensive understanding to genetic risk prediction. *Mol Psychiatry*. 2012;17:887–905.
  53. Teyssier JR, Ragot S, Chauvet-Gelinier JC, Trojak B, Bonin B. Activation of a  $\Delta$ FOSB dependent gene expression pattern in the dorsolateral prefrontal cortex of patients with major depressive disorder. *J Affect Disord*. 2011;133:174–178.
  54. Araya-Callis C, Hiemke C, Abumaria N, Flugge G. Chronic psychosocial stress and citalopram modulate the expression of the glial proteins GFAP and NDRG2 in the hippocampus. *Psychopharmacology (Berl)*. 2012;224:209–222.
  55. Boulkroun S, Fay M, Zennaro MC, et al. Characterization of rat NDRG2 (N-Myc downstream regulated gene 2), a novel early mineralocorticoid-specific induced gene. *J Biol Chem*. 2002;277:31506–31515.
  56. Hoo RL, Chu JY, Yuan Y, Yeung CM, Chan KY, Chow BK. Functional identification of an intronic promoter of the human glucose-dependent insulinotropic polypeptide gene. *Gene*. 2010;463:29–40.
  57. Meyer MB, Goetsch PD, Pike JW. Genome-wide analysis of the VDR/RXR cisome in osteoblast cells provides new mechanistic insight into the actions of the vitamin D hormone. *J Steroid Biochem Mol Biol*. 2010;121:136–141.
  58. Ott CJ, Blackledge NP, Leir SH, Harris A. Novel regulatory mechanisms for the CFTR gene. *Biochem Soc Trans*. 2009;37:843–848.
  59. Vazquez BN, Laguna T, Notario L, Lauzurica P. Evidence for an intronic cis-regulatory element within CD69 gene. *Genes Immun*. 2012;13:356–362.
  60. Bosia C, Osella M, El BM, Cora D, Caselle M. Gene autoregulation via intronic microRNAs and its functions. *BMC Syst Biol*. 2012;6:131.
  61. Gromak N. Intronic microRNAs: a crossroad in gene regulation. *Biochem Soc Trans*. 2012;40:759–761.
  62. Ovcharenko I, Loots GG, Nobrega MA, Hardison RC, Miller W, Stubbs L. Evolution and functional classification of vertebrate gene deserts. *Genome Res*. 2005;15:137–145.
  63. Bagamasbad P, Ziera T, Borden SA, et al. Molecular basis for glucocorticoid induction of the Kruppel-like factor 9 gene in hippocampal neurons. *Endocrinology*. 2012;153:5334–5345.
  64. Ma Y, Wu X, Li X, et al. Corticosterone regulates the expression of neuropeptide Y and reelin in MLO-Y4 cells. *Mol Cells*. 2012;33:611–616.
  65. Sapolsky RM, Romero LM, Munck AU. How do glucocorticoids influence stress responses? Integrating permissive, suppressive, stimulatory, and preparative actions. *Endocr Rev*. 2000;21:55–89.
  66. Trapp T, Rupprecht R, Castren M, Reul JM, Holsboer F. Heterodimerization between mineralocorticoid and glucocorticoid receptor: a new principle of glucocorticoid action in the CNS. *Neuron*. 1994;13:1457–1462.
  67. Nishi M, Tanaka M, Matsuda K, Sunaguchi M, Kawata M. Visualization of glucocorticoid receptor and mineralocorticoid receptor interactions in living cells with GFP-based fluorescence resonance energy transfer. *J Neurosci*. 2004;24:4918–4927.
  68. Datson NA, van der Perk J, de Kloet ER, Vreugdenhil E. Identification of corticosteroid-responsive genes in rat hippocampus using serial analysis of gene expression. *Eur J Neurosci*. 2001;14:675–689.
  69. Yang PC, Yang CH, Huang CC, Hsu KS. Phosphatidylinositol 3-kinase activation is required for stress protocol-induced modification of hippocampal synaptic plasticity. *J Biol Chem*. 2008;283:2631–2643.
  70. Costello DA, Claret M, Al-Qassab H, et al. Brain deletion of insulin receptor substrate 2 disrupts hippocampal synaptic plasticity and metaplasticity. *PLoS One*. 2012;7:e31124.
  71. Schaaf MJ, Lewis-Tuffin LJ, Cidlowski JA. Ligand-selective targeting of the glucocorticoid receptor to nuclear subdomains is associated with decreased receptor mobility. *Mol Endocrinol*. 2005;19:1501–1515.
  72. Ravasi T, Suzuki H, Cannistraci CV, et al. An atlas of combinatorial transcriptional regulation in mouse and man. *Cell*. 2010;140:744–752.
  73. Igreja C, Izaurralde E. CUP promotes deadenylation and inhibits decapping of mRNA targets. *Genes Dev*. 2011;25:1955–1967.
  74. Jonat C, Rahmsdorf HJ, Park KK, et al. Antitumor promotion and antiinflammation: down-modulation of AP-1 (Fos/Jun) activity by glucocorticoid hormone. *Cell*. 1990;62:1189–1204.
  75. De Bosscher K, Van Craenenbroeck K, Meijer OC, Haegeman G. Selective transrepression versus transactivation mechanisms by glucocorticoid receptor modulators in stress and immune systems. *Eur J Pharmacol*. 2008;583:290–302.
  76. Chebotaev D, Yemelyanov A, Budunova I. The mechanisms of tumor suppressor effect of glucocorticoid receptor in skin. *Mol Carcinog*. 2007;46:732–740.
  77. Glass CK, Saijo K. Nuclear receptor transrepression pathways that regulate inflammation in macrophages and T cells. *Nat Rev Immunol*. 2010;10:365–376.